ATMOSPHERIC SCIENCE LETTERS
RMetS Royal Meteorological Society

Sensitivity of tropical deep convection in global models: effects of horizontal resolution, surface constraints and 3D atmospheric nudging

Journal:	*Atmospheric Science Letters*
Manuscript ID:	ASL-14-064.R1
Wiley - Manuscript type:	Research Article
Date Submitted by the Author:	n/a
Complete List of Authors:	Chemel, Charles Russo, Maria Hosking, Scott Telford, Paul Pyle, John
Keywords:	tropical deep convection, global models, nudging, surface fluxes

Sensitivity of tropical deep convection in global models: effects of horizontal resolution, surface constraints and 3D atmospheric nudging

(Short running title: Tropical Deep Convection in Global Models)

Charles Chemel[1]*, Maria R. Russo[2,3], J. Scott Hosking[2,4], Paul J. Telford[2,3], and John A. Pyle[2,3]

[1]*National Centre for Atmospheric Science (NCAS Weather), Centre for Atmospheric & Instrumentation Research, University of Hertfordshire, College Lane, Hatfield, AL10 9AB, UK*

[2]*Centre for Atmospheric Science, Department of Chemistry, University of Cambridge, Lensfield Road, Cambridge, CB2 1EW, UK*

[3]*National Centre for Atmospheric Science (NCAS Climate), Centre for Atmospheric Science, Department of Chemistry, University of Cambridge, Lensfield Road, Cambridge, CB2 1EW, UK*

[4]*Now at British Antarctic Survey, NERC, Madingley Road, High Cross, Cambridge, CB3 0ET, UK*

**Correspondence to: Charles Chemel, Centre for Atmospheric & Instrumentation Research, University of Hertfordshire, College Lane, Hatfield, AL10 9AB, UK. E-mail: c.chemel@herts.ac.uk*

Abstract

We investigate the ability of global models to capture the spatial patterns of tropical deep convection. Their sensitivity is assessed through changing horizontal resolution, surface flux constraints, and constraining background atmospheric conditions. We assess two models at typical climate and weather forecast resolutions. Comparison with observations indicates that increasing resolution generally improves the pattern of tropical convection. When the models are constrained with realistic surface fluxes and atmospheric structure, the location of convection improves dramatically and is very similar irrespective of resolution and parameterisations used in the models.

Keywords: tropical deep convection; global models; nudging; surface fluxes

1. Introduction

Tropical deep convection plays an important role in determining the dynamics and composition of the atmosphere in both the tropics and extra-tropics over a broad range of spatial and temporal scales. For long climate simulations, and the study of chemistry-climate interactions, tropical deep convection is key for a correct representation of (i) a realistic distribution of high clouds and associated changes in the radiative balance of the atmosphere (e.g., Ramanathan *et al.*, 1989), (ii) the vertical transport of pollutants and water vapour to the upper troposphere and lower stratosphere (Holton *et al.*, 1995), and

(iii) coupling to large-scale dynamics through gravity waves and modulation of the Madden-Julian oscillation (Zhang, 2005). The fast vertical transport of very short-lived brominated substances by deep tropical storms is also potentially important for the recovery of the stratospheric ozone layer over the coming century (Yang *et al.*, 2014). In the context of numerical weather predictions, the location, timing and intensity of tropical deep convection are important for a reliable forecast of severe storms and associated natural hazards. Getting a realistic representation of tropical deep convection is therefore a crucial issue for both global forecast runs and climate and Earth-system simulations.

Although several sub-grid scale convection parameterisation schemes have been developed, their ability to represent convection has been shown to be highly dependent on the resolution of the host model (e.g., Brankovic and Gregory, 2001). This is linked to the inability of coarse resolutions to properly represent geographical features which have been shown to be strongly linked to convection; these include proper representation of coastlines (Schiemann *et al.*, 2014), orography (Kirshbaum and Smith, 2009) and land use (Anthes, 1984). Furthermore, coarse resolution models fail to resolve small-scale dynamical features such as sea breezes, one of the triggering mechanisms for convection in coastal areas (Qian, 2008). In addition to the above effects driven by model resolution, convection parameterisation schemes rely on the host model to provide a realistic distribution of heat and moisture fluxes at the surface, which are in turn dependent on surface characteristics such as temperature, soil moisture (Taylor *et al.*, 2012) and winds. These fluxes often determine the initial stages of convection development, particularly for continental convection (e.g., over Africa), where soil moisture is crucial in driving the formation of shallow cumulus clouds (Ek and Holtslag, 2004). After this initial stage, the transition between shallow and deep convection depends on the vertical structure of the air column and the measure of its instability, and therefore convection parameterisation schemes also rely on the host model to provide a realistic three-dimensional (3D) structure of the atmosphere (Martin *et al.*, 2010).

Our aim is to investigate the ability of models with parameterised convection to represent the location and intensity of tropical deep convection over varying scales and with varying constraints. We use two models, the Weather Research and Forecasting (WRF) modelling system (Skamarock *et al.*, 2008), and the UK Met Office Unified Model (MetUM) (Davies *et al.*, 2005). We quantify the model ability to match the observed monthly mean pattern of tropical deep convection and examine the relative importance of horizontal resolution, surface fluxes and 3D state of the atmosphere, and how their changes affect model convection.

2. Methodology and data

In this section we describe the convection parameterisations used for this study, the set-up of the numerical experiments, and the observational data and statistical techniques used for the model evaluation. The sub-grid scale effects of convection were parameterised using the ensemble cumulus

scheme of Grell and Dévényi (2002) in WRF and the mass flux convection scheme of Gregory and Rowntree (1990) in MetUM. For a detailed description of WRF and MetUM the reader is directed to Skamarock *et al.* (2008) and Davies *et al.* (2005), respectively. Static characteristics of the land surface (such as orography, vegetation and soil types) were derived from the default geographical datasets provided with each model.

We run the two models using the same four horizontal resolutions, namely N48 (3.75ºx2.50º), N96 (1.87ºx1.25º), N144 (1.25ºx0.83º), and N216 (0.83ºx0.56º); the vertical resolution is kept the same and is defined similarly in the two modelling systems, i.e. 38 vertical levels up to 5 hPa for WRF and up to about 40 km for MetUM, giving a vertical resolution of about 1 km in the upper troposphere/lower stratosphere region. The WRF experiments used the same physics options for all horizontal resolutions, while the MetUM experiments are based on the HadGAM climate setup (Martin *et al.*, 2006) for coarse resolutions (N48 and N96), and on the UK Met Office operational global forecast setup (Petch *et al.*, 2007) for higher resolutions (N144 and N216). In order to minimise the impact of synoptic scale model biases, we initialise model simulations to analysis and integrate the models over a relatively short timescale (1 month), similar to the approach used for instance in Stock *et al.* (2014). All experiments are run for a neutral El Niño–Southern Oscillation year, specifically for the months of July and November 2005, which exhibit convection patterns typical of the summer and winter seasons, respectively (see Section 3). Otherwise, there is no particular reason for the selection of these two months. The initial conditions are derived from the European Centre for Medium-range Weather Forecasts (ECMWF) operational analyses for WRF, and from the UK Met Office data-assimilated start dumps for MetUM.

For each model resolution we ran 3 sets of experiments:

- *Sea only*: sea surface temperature and sea ice are updated daily to observed values: for MetUM and WRF we use data from the AMIP dataset (AMIP-II; Gates *et al.*, 1999) and ECMWF operational analyses, respectively. Heat and moisture fluxes over land are determined by the interaction of the atmosphere with soil moisture and soil temperature calculated by the land surface scheme.
- *Sea + Land*: sea surface temperature and sea ice are treated as described above, while heat and moisture fluxes over land are constrained as follows: in WRF the first (surface) atmospheric layer is nudged towards ECMWF temperature and water vapour with a relaxation timescale of 1 hour (see Stauffer and Seaman, 1990, for details on the nudging technique); in MetUM, since there is no option in the model for nudging below the free troposphere, soil temperature and soil moisture are updated daily from a climatological dataset provided with the model release.
- *Nudged*: these runs apply the same surface constraints as the *Sea + Land* runs; additionally the 3D structure of the free troposphere is constrained by nudging horizontal winds and temperature

towards ECMWF operational analyses. We only performed *Nudged* runs for MetUM at N48 resolution; technical details on the nudging technique are described in Telford *et al.* (2008).

In order to evaluate the different model runs we compare the model monthly mean outgoing long-wave radiation (OLR) and precipitation rate (PR) to observations. OLR is commonly used to identify the presence of cold cloud tops, which are linked to high clouds produced by tropical deep convection (e.g., Arkin and Ardanuy, 1989). We use monthly mean OLR to identify geographical areas of recurrent convection and the estimated depth of the convection. Monthly mean OLR and PR, used in combination, are a good proxy for the location and intensity of recurrent tropical deep convection (Hosking *et al.*, 2010; Russo *et al.*, 2011). The model OLR is compared to those derived from the AVHRR instrument on board NOAA polar-orbiting satellites (Gruber and Krueger, 1984) and from the AIRS instrument on board the EOS Aqua satellite (Aumann *et al.*, 2003), available as gridded products with a grid resolution of 2.5ºx2.5º and 1ºx1º, respectively. The model PR is compared to values from the CPC Merged Analysis of Precipitation (CMAP) standard (Huffman *et al.*, 1997), the Global Precipitation Climatology Project (GPCP) 1DD (Huffman *et al.*, 2001), and the Tropical Rainfall Measuring Mission (TRMM) 3A12 (Kummerow *et al.*, 1998) products, available as gridded products with a grid resolution of 2.5ºx2.5º, 1ºx1º and 0.5ºx0.5º, respectively. The model and observed monthly mean OLR and PR data is then degraded to the coarsest product resolution (2.5ºx2.5º) and for each model simulation we calculate the spatial correlation and the coefficient of variation of the root mean square error (CVRMSE) between modelled and observed OLR and PR. The spatial correlation r (calculated using Pearson correlation coefficient) gives a measure of the linear relationship between models and observations. A value close to one indicates that model and observations have very similar spatial patterns, although model biases are not picked up using this metric. The CVRMSE (defined as the root mean square error relative to the observed mean) is used as a complementary metric to estimate how accurately a model can reproduce the observed magnitude of a specific variable. A value closer to zero indicates better agreement between model and observations. The combination of these two metrics provides a measure of the models ability to represent the geographical location (measured by r) and intensity (measured by CVRMSE) of tropical deep convection.

3. Results and discussion

Correlation coefficients and CVRMSE between the AIRS and TRMM products and both the model and the other observational datasets are calculated for the *Tropics* (20ºS–20ºN) and the tropical *Land* and *Sea* areas, respectively (see Tables S1 to S4). The two observed OLR are in very good agreement, with correlation coefficients greater than 0.97 and CVRMSE of about 7.5% for the *Tropics*. In contrast, the agreement between the three observed PR datasets is not as good, with correlation coefficients between r = 0.87 and 0.92 and CVRMSE greater than 47% for the *Tropics*. Explaining

the differences between the different observational products is out of the scope of the present work. In the following, we use the correlation coefficients and CVRMSE between different observational datasets as a reference value to measure the strength of the agreement between models and observations: we then define 'very good agreement' and 'good agreement' with observations if the modelled r or CVRMSE are respectively within 10% and 20% of our reference values. The use of monthly mean data ensures that the emphasis of this analysis is not on the models ability to represent single convective events but rather on their ability to represent the effects of convection at the monthly mean scale.

We now investigate the models ability to represent the observed geographical location of tropical convection. Analysis of the correlation coefficients in table S1-S4 shows that overall ~70% of the model configurations are in good agreement with observations over the Tropics. However, there is a much better agreement between modelled and observed values for OLR (~90% of model configurations are in good agreement with observations) than for PR (only ~45% of model configurations are in good agreement with observations). Similarly, the percentage of models in good agreement with observations is larger for the month of July (~80%) than November (~55%). There is also a small difference in the models ability to represent convection over land than over sea: the percentage of model configurations in good agreement with observations is ~85% and ~60% respectively for land and sea).

After looking at the geographical location of convection, we now address how well the models can represent the intensity of tropical convection. Analysis of CVRMSE values in Tables S1 to S4 shows that model errors over the tropics are generally small for OLR and much larger for PR. This is in agreement with previous studies, which show large model precipitation biases in tropical ocean regions (Martin *et al.*, 2010; Schiemann *et al.*, 2014). For OLR ~85% of model configurations are in good agreement with observations while for PR none of the models are in good agreement with observations, with values of CVRMSE around a factor of two larger than the values between different observations. Differences in model performance between different months or between land and sea areas are negligible, indicating that models are much better at representing the physical processes that link convection to OLR while they struggle to satisfactorily represent the processes linking tropical convection to the intensity of precipitation, although changes in the parameterisation scheme have shown to significantly improve these biases (Martin et al. 2010).

We now specifically address the effect of increasing model constraints, as illustrated in Figure 1. For this purpose we use the MetUM runs at N48 resolution for November 2005. Figures 1a and 1b show observed OLR and PR for November 2005, and highlight the three main wintertime tropical convective regions: sub-Saharan Africa, the Eastern Indian Ocean and Maritime Continent, and tropical South America. The Inter Tropical Convergence Zone (ITCZ), and to a smaller extent the South Pacific Convergence Zone (SPCZ), also have their signatures in the OLR and PR fields. When the model is constrained only at the surface, the OLR and PR fields show some unrealistic convective

features, for instance over most of the Indian Ocean and off the East coast of Africa, compared to those observed. Despite adding the constraints over *Land* areas, the correlation coefficients between modelled and observed values over the *Tropics* are similar for the *Sea only* and *Sea + Land* runs and none of the model configurations is in good agreement with observations (r = 0.73 and 0.76 for OLR, and r = 0.66 and 0.67 for PR, respectively). Comparison of the correlation coefficients for *Sea only* and *Sea + Land* runs shows a similar behaviour for all MetUM resolutions, with generally similar correlation coefficients for *Land* values when land constraints are applied and only small differences in the correlation for the *Tropics*. To explain the lack of improvement of MetUM to adding the surface constraints over *Land* areas, we analysed monthly mean water vapour at 20 m (not shown). Constraining soil moisture and soil temperature produces only small changes to the surface water vapour, indicating that monthly mean fluxes of heat and moisture over land are well represented by the coupling between the atmosphere and land surface scheme. When the state of the atmosphere is constrained by nudging towards operational analyses, the pattern of convection improves significantly, both over *Land* and *Sea* areas, and correlation coefficients for the *Tropics* of show very good agreement for OLR and good agreement for PR (r = 0.89 and 0.74, respectively). The analysis of data from WRF model runs shows that the sensitivity of the model to changes in constraints for a given resolution is very similar to that of MetUM, with a significant improvement in performance for the *Nudged* runs only (see Tables S1 to S4). Overall, the location of convection is in very good agreement with observations in ~60% of *Nudged* runs as opposed to ~10% of the runs where only surface constraints are applied. This highlights the importance of a realistic structure of the atmosphere and global circulation patterns in representing the location and intensity of tropical deep convection.

The sensitivity of both MetUM and WRF to changes in horizontal resolution is also very similar. The effect of increasing horizontal resolution is illustrated in Figure 2. For this purpose we choose the WRF model simulations for July 2005 with the least constraints, i.e. the *Sea only* runs, for which the benefit of increasing model resolution is expected to be the largest. Figures 2a and 2b show the observed convection patterns typical of the northern hemisphere summer season, with convective regions mostly north of the Equator, for example sub-Saharan Africa, the ITCZ and SPCZ, and the strong Asian and the North American monsoon. Figure 2 shows that the main convective areas are well captured, although the model SPCZ is less visible than that observed. Tables S1 and S3 show a consistent improvement as WRF model resolution is increased from N48 to N216, with correlation coefficients of r = 0.84 and 0.88 for OLR, and r = 0.69 and 0.73 for PR, and CVRMSE of 7.2 and 5.7% for OLR, and 91 and 85% for PR, respectively. The sensitivity of MetUM to changes in horizontal resolution is also very similar. Overall, correlation coefficients in Tables S1 to S4 show that ~80% of N216 model configurations are in good agreement with observations, as opposed to ~60% for N48, and these change to ~70% and ~40% when *Nudged* runs are not included. The gain in WRF performance with resolution is of the same order for the *Sea + Land* runs. This indicates that the

improvement from increasing resolution is mainly the result of a better representation of small-scale dynamical features in *Sea* areas (such as low level convergence leading to the ITCZ, and sea breezes leading to convection in coastal areas). However, for the *Nudged* runs, where the model surface and free troposphere are both constrained, only the CVRMSE values are significantly reduced as model resolution is increased, while the difference in the correlation coefficients becomes almost negligible, indicating that the intensity of convection can still be improved by increasing resolution, while the location of convection in the *Nudged* runs is well captured even at the coarsest resolution.

4. Conclusions

Figure 3 summarises the effect of increasing resolution and constraints on the model ability to reproduce the observed pattern of convection for the two models in both seasons.

The sensitivity of both models to horizontal resolution is reflected by a general improvement going from N48 to N216. For example, Figure 4a shows how increasing horizontal resolution for the MetUM *Sea only* runs leads to an improvement in the correlation coefficients between modelled and observed OLR, and Figure 4b shows that the errors decrease for the same model runs as the resolution increases from N48 to N216. This is generally true for both models and for both sets of runs using surface constraints (*Sea only* and *Sea + Land*). However, for *Nudged* runs, where constraints are applied throughout the atmospheric column, the improvement resulting from increased resolution is much smaller and is generally notable only in the intensity of convection (as measured by the CVRMSE values).

Both models show very little change when increasing the surface constraint from *Sea only* to *Sea + Land*, while a significant improvement in performance (higher correlation coefficients and lower CVRMSE) is notable for the *Nudged* runs, where the model surface and free troposphere are both constrained. Furthermore, the similar performance of *Nudged* WRF and MetUM runs indicates that when the surface fluxes and 3D structure of the host model are constrained, the ability to represent the preferential location of tropical deep convection is almost insensitive to the parameterisations used, including the convection parameterisation scheme. However, note that both surface fluxes and 3D atmospheric structure can also be affected by convection, as well as being crucial in determining its onset and development; it is therefore difficult to truly disentangle the extent to which errors in the representation of convection are due to biases introduced by the convection parameterisation itself (e.g. through positive feedbacks in radiation and precipitation/evaporation) or to biases arising from other model components.

Additionally, for the *Nudged* runs, the major impact of convection on temperature and moisture through condensation and latent heat release is strongly constrained and therefore one must not conclude that current convection parameterisation schemes are able to reproduce the observed intensity of tropical convection.

Supporting information

Table S1. July 2005 monthly correlation coefficients and CVRMSE for OLR.

Table S2. July 2005 monthly correlation coefficients and CVRMSE for PR.

Table S3. November 2005 monthly correlation coefficients and CVRMSE for OLR.

Table S4. November 2005 monthly correlation coefficients and CVRMSE for PR.

Acknowledgments

The research was funded by the UK Natural Environment Research Council (NERC) and the UK National Centre for Atmospheric Science (NCAS). PJT acknowledges the UK National Centre for Earth Observation (NCEO) for funding. JSH gratefully acknowledges an e-Science PhD studentship by NERC. Model simulations were performed on the UK national supercomputing facilities (HECToR), accessed through NCAS. This work was conducted while CC was a visiting researcher at the Centre for Atmospheric Science, Department of Chemistry, University of Cambridge, Lensfield Road, Cambridge, CB2 1EW, UK.

References

Anthes RA. 1984. Enhancement of convective precipitation by mesoscale variations in vegetative covering in semiarid regions. *Journal of Climate and Applied Meteorology* **23**: 541–554.

Arkin PA, Ardanuy PE. 1989. Estimating climatic-scale precipitation from space: A review. *Journal of Climate* **2**: 1229–1238.

Aumann HH, Chahine MT, Gautier C, Goldberg MD, Kalnay E, McMillan LM, Revercomb H, Rosenkranz PW, Smith WL, Staelin DH, Strow LL, Susskind J. 2003. AIRS/AMSU/HSB on the Aqua mission: Design, science objectives, data products, and processing systems. *IEEE Transactions on Geoscience and Remote Sensing* **41**: 253–264.

Brankovic C, Gregory D. 2001. Impact of horizontal resolution on seasonal integrations. *Climate Dynamics* **18**: 123–143.

Davies T, Cullen MJP, Malcolm AJ, Mawson MH, Staniforth A, White AA, Wood N. 2005. A new dynamical core for the Met Office's global and regional modelling of the atmosphere. *Quarterly Journal of the Royal Meteorological Society* **131**: 1759–1782.

Ek MB, Holtslag AAM. 2004. Influence of soil moisture on boundary layer cloud development. *Journal of Hydrometeorology* **5**: 86–99.

Gates WL, Boyle JS, Covey C, Dease CG, Doutriaux CM, Drach RS, Fiorino M, Gleckler PJ, Hnilo JJ, Marlais SM, Phillips TJ, Potter GL, Santer BD, Sperber KR, Taylor KE, Williams DN. 1999. An overview of the results of the Atmospheric Model Intercomparison Project (AMIP I). *Bulletin of the American Meteorological Society* **80**: 29–55.

Gregory D, Rowntree PR. 1990. A mass flux convection scheme with representation of cloud ensemble characteristics and stability-dependent closure. *Monthly Weather Review* **118**: 1483–1506.

Grell GA, Dévényi D. 2002. A generalized approach to parameterizing convection combining ensemble and data assimilation techniques. *Geophysical Research Letters* **29**: Art. No. 1693. DOI:10.1029/2002GL015311.

Gruber A, Krueger AF. 1984. The status of the NOAA outgoing longwave radiation data set. *Bulletin of the American Meteorological Society* **65**: 958–962.

Holton JR, Haynes PH, McIntyre ME, Douglass AR, Rood RB, Pfister L. 1995. Stratosphere-troposphere exchange. *Reviews of Geophysics* **33**: 403–440.

Hosking JS, Russo MR, Braesicke P, Pyle JA. 2010. Modelling deep convection and its impacts on the tropical tropopause layer. *Atmospheric Chemistry and Physics* **10**: 11175–11188.

Huffman GJ, Adler RF, Arkin P, Chang A, Ferraro R, Gruber A, Janowiak J, McNab A, Rudolf B, Schneider U. 1997. The Global Precipitation Climatology Project (GPCP) combined data set. *Bulletin of the American Meteorological Society* **78**: 5–20.

Huffman GJ, Adler RF, Morrissey M, Bolvin DT, Curtis S, Joyce R, McGavock B, Susskind J. 2001. Global precipitation at one-degree daily resolution from multi-satellite observations. *Journal of Hydrometeorology* **2**: 36–50.

Kirshbaum DJ, Smith RB. 2009. Orographic precipitation in the tropics: large-eddy simulations and theory. *Journal of the Atmospheric Sciences* **66**: 2559–2578.

Kummerow C, Barnes W, Kozu T, Shiue J, Simpson J. 1998. The Tropical Rainfall Measuring Mission (TRMM) sensor package. *Journal of Atmospheric and Oceanic Technology* **15**: 808–816.

Martin GM, Ringer MA, Pope VD, Jones A, Dearden C, Hinton TJ. 2006. The physical properties of the atmosphere in the new Hadley Centre Global Environmental Model (HadGEM1). Part I: Model description and global climatology. *Journal of Climate* **19**: 1274–1301.

Martin GM, Milton SF, Senior CA, Brooks ME, Ineson S, Reichler T, Kim J. 2010. Analysis and reduction of systematic errors through a seamless approach to modelling weather and climate. *Journal of Climate* **23**: 5933–5957.

Petch JC, Willett M, Wong RY, Woolnough SJ. 2007. Modelling suppressed and active convection. Comparing a numerical weather prediction, cloud-resolving and single-column model. *Quarterly Journal of the Royal Meteorological Society* **133**: 1087–1100.

Qian J-H. 2008. Why precipitation is mostly concentrated over islands in the Maritime Continent. *Journal of the Atmospheric Sciences* **65**: 1428–1441.

Ramanathan V, Cess RD, Harrison EF, Minnis P, Barkstrom BR, Ahmad E, Hartmann D. 1989. Cloud-radiative forcing and climate: Results from the Earth Radiation Budget Experiment. *Science* **243**: 57–63.

Russo MR, Marécal V, Hoyle CR, Arteta J, Chemel C, Chipperfield MP, Dessens O, Feng W, Hosking JS, Telford PJ, Wild O, Yang X, Pyle JA. 2011. Representation of tropical deep convection in atmospheric models – Part 1: Meteorology and comparison with satellite observations. *Atmospheric Chemistry and Physics* **11**: 2765–2786.

Schiemann R, Demory M-E, Mizielinski MS, Roberts MJ, Shaffrey LC, Strachan J, Vidale PL. 2014. The sensitivity of the tropical circulation and Maritime Continent precipitation to climate model resolution. *Climate Dynamics* **42**: 2455–2468.

Skamarock WC, Klemp JB, Dudhia J, Gill DO, Barker DM, Duda MG, Huang X-Y, Wang W, Powers JG. 2008. A description of the Advanced Research WRF Version 3. The National Center for Atmospheric Research: Boulder, CO, USA (NCAR Technical Note NCAR/TN-475+STR).

Stauffer DR, Seaman, N. 1990. Use of Four-Dimensional Data Assimilation in a limited-area mesoscale model. Part I: Experiments with synoptic-scale data. *Monthly Weather Review* **118**: 1250–1277.

Taylor CM, de Jeu RAM, Guichard F, Harris PP, Dorigo WA. 2012. Afternoon rain more likely over drier soils. *Nature* **489**: 423–6.

Telford PJ, Braesicke P, Morgenstern O, Pyle JA. 2008. Technical Note: Description and assessment of a nudged version of the new dynamics Unified Model. *Atmospheric Chemistry and Physics* **8**: 1701–1712.

Yang X, Abraham NL, Archibald AT, Braesicke P, Keeble J, Telford P, Warwick NJ, Pyle JA. 2014. How sensitive is the recovery of stratospheric ozone to changes in concentrations of very short lived bromocarbons? *Atmospheric Chemistry and Physics Discussions* **14**: 9729–9745.

Zhang CD. 2005. Madden-Julian Oscillation. *Reviews of Geophysics* **43**: Art. No. RG2003. DOI:10.1029/2004RG000158.

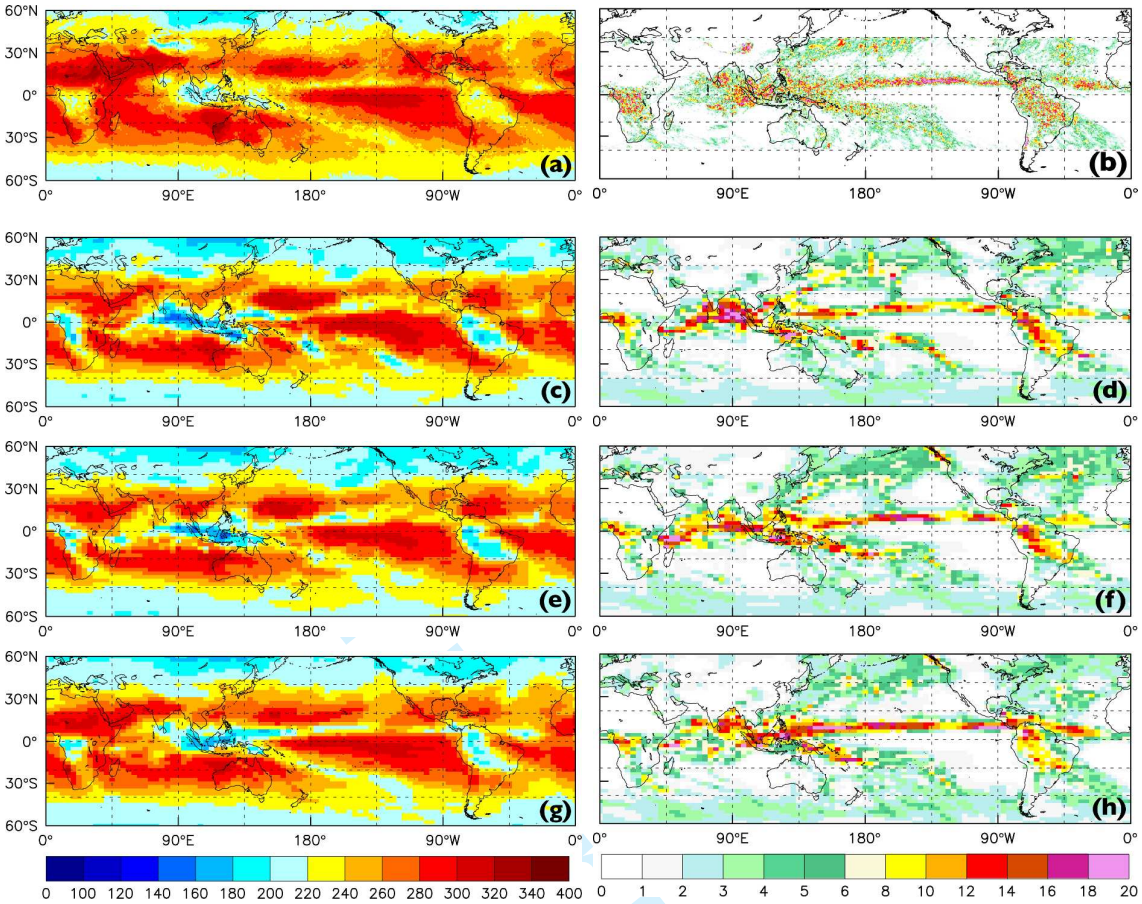

Figure 1. Monthly mean maps of outgoing long-wave radiation (OLR) in W m^{-2} (left) and precipitation rate (PR) in mm d^{-1} (right) for November 2005 from the AIRS (a) and TRMM (b) products, and the MetUM N48: (a) and (b) *Sea only*, (c) and (d) *Sea + Land*, and (e) and (f) *Nudged* runs.

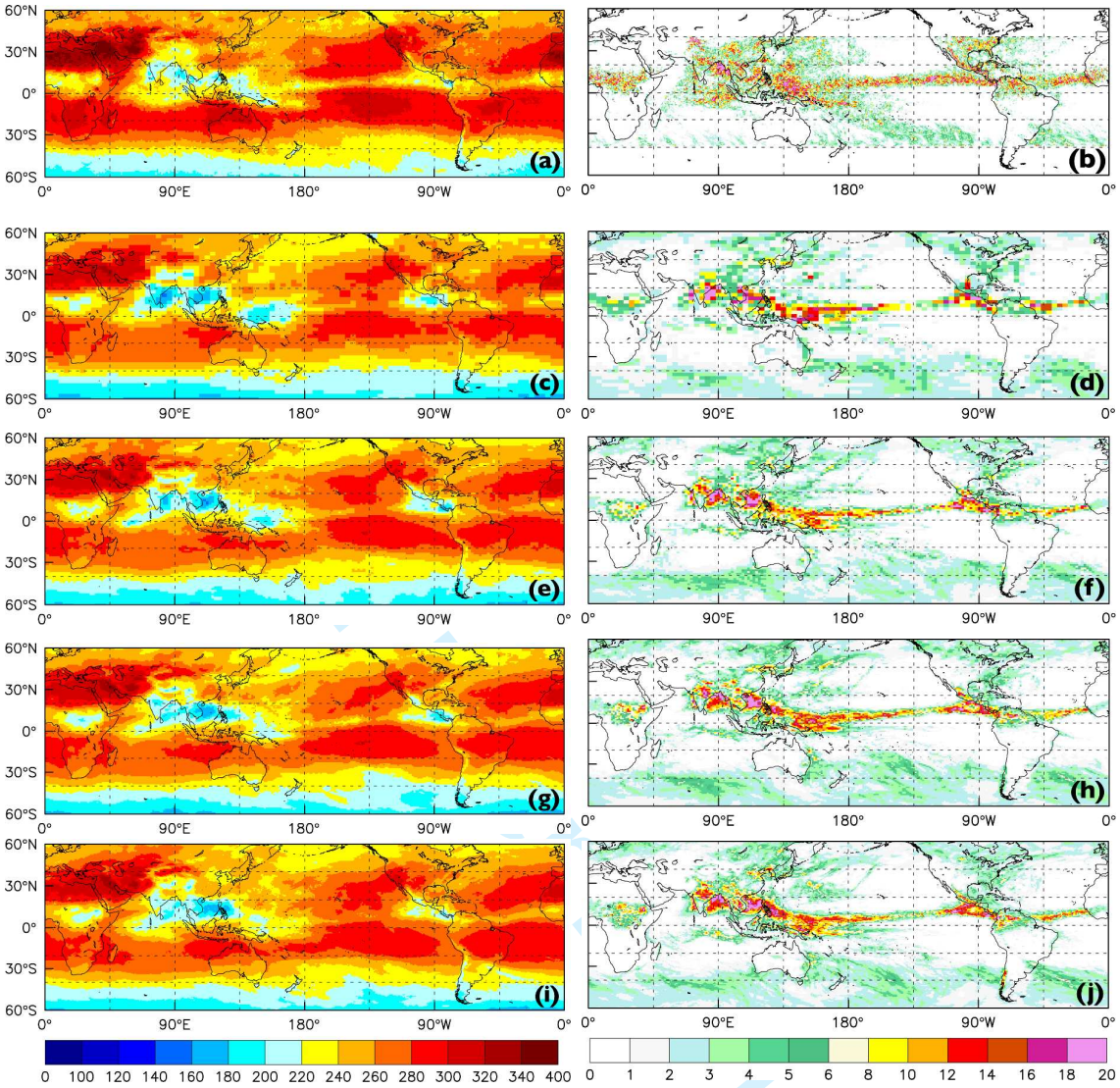

346 **Figure 2.** Monthly mean maps of outgoing long-wave radiation (OLR) in W m^{-2} (left) and
347 precipitation rate (PR) in mm d^{-1} (right) for July 2005 from the AIRS (a) and TRMM (b)
348 products, and from the WRF *Sea only* runs at: (a) and (b) N48, (c) and (d) N96, (e) and (f)
349 N144, and (g) and (h) N216 resolutions.

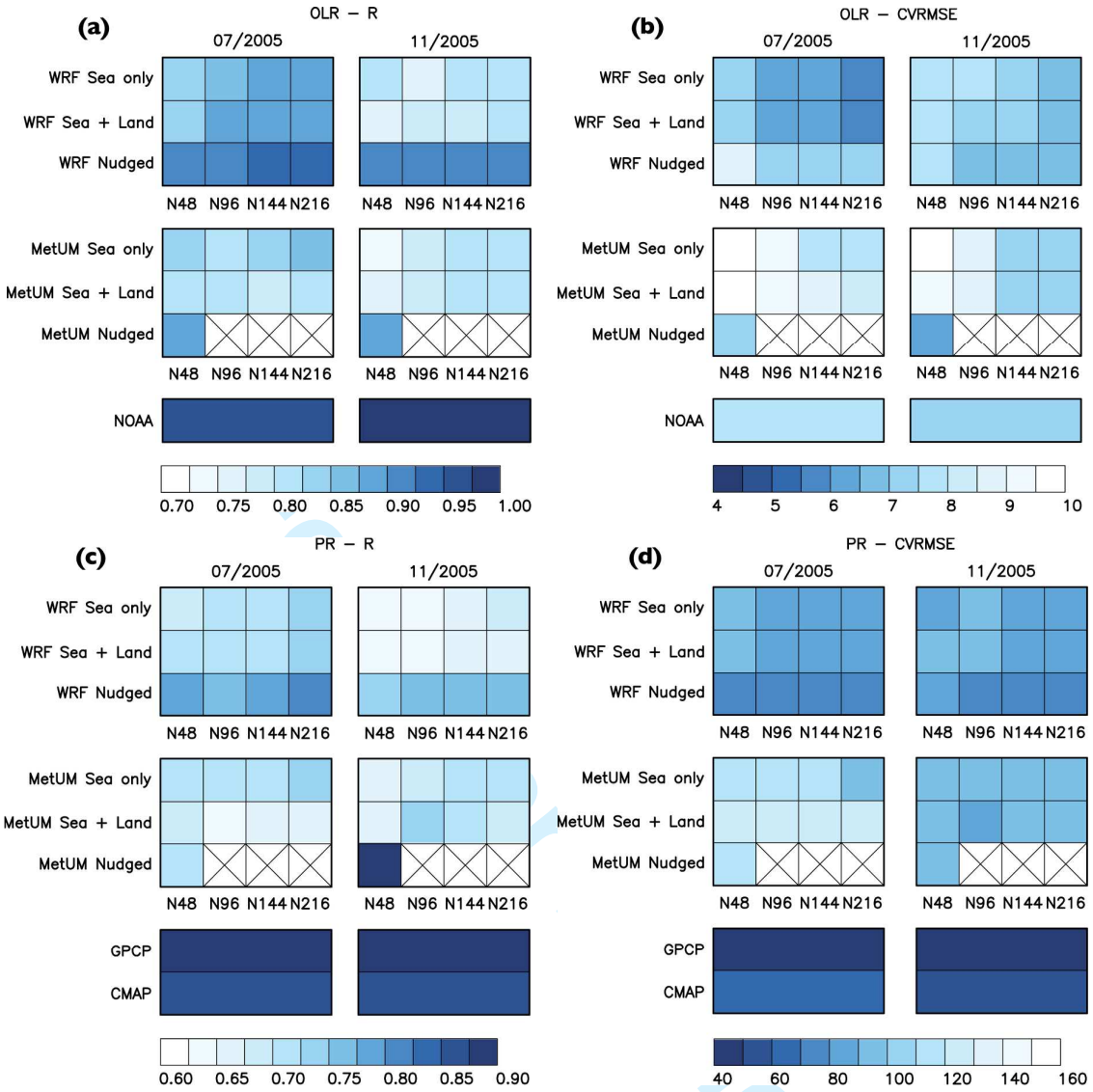

Figure 3. Matrix plots of correlation coefficients (left) and CVRMSE in % (right) between modelled and observed values over the *Tropics* (20ºS–20ºN) for July and November 2005, calculated against the AIRS and TRMM datasets for (a) and (b) outgoing long-wave radiation (OLR) and (c) and (d) precipitation rate (PR), respectively.